

INFERRED TWO-DIMENSIONAL SPATIAL CURRENT DENSITY DISTRIBUTION FROM MAGNETIC SOURCES

Akala A. O.

Department of Physics, University of Lagos, Akoka, Yaba, Lagos, Nigeria

Abstract

The use of imaging has usually be an essential aspect of scientific investigations and medical diagnoses. In the applications of imaging for the above stated investigations and diagnoses, achieving optimal resolution of the reconstructed images is of prime importance. In this study, the magnetic inverse problem was solved via Fourier transforms to reconstruct two-dimensional current mappings. The dimensions of the conducting sheet, upon which the current density is to be reconstructed, as well as the distance of the magnetic source to the conducting sheet were varied, and the corresponding images of the current density were reconstructed. The thickness of a conducting sheet determines the spatial current density distributions and image resolutions. The spatial resolutions of the reconstructed current density images were higher at nanometer and micrometer scale magnetic source distance to the conducting sheet, and blurred at a millimeter scale distance.

1.0 Introduction

Imaging is an essential aspect of scientific and medical investigations/diagnoses [1, 2]. Many applications of imaging techniques abounds, some of which are; optical microscopy, x-rays, ultrasound, magnetic resonance, among others. For instance, at micro and nano scales, Xing et al. [3] used scanning Hall probes to reconstruct current density mapping. Johansen et al. [4] adopted magnetoresistance probes technique for current density mapping reconstruction. Whereas, authors, such as, Schrag and Xiao [5] used magneto-optical methods for current density mapping. Baudenbacher et al. [2] and Holzer et al. [6] reconstructed high resolution images of currents in human cardiac tissue from biomagnetic fields. On the other hand, some authors have reconstructed good resolution images by a combined method of magnetoresistance and spin filters [7, 8, 9].

Another prominent imaging technique that has found wide range applications in many areas of human endeavour is the Superconducting Quantum Interference Devices (SQUIDS) [1, 10]. For two-dimensional analyses, the formulation of the above named techniques is usually based on the fact that a current density map can be reconstructed from a single component of the magnetic field that is recorded in a plane at a fixed distance over the current sheet [11]. This process is known as the magnetic inversion technique. Lately, magnetic inversion technique is gaining widespread applications in nanotechnology [12, 13, 14].

In this study, the magnetic inverse problem was solved for two-dimensional current mappings by using Fourier transforms, with a view to determining the relationships between the distance where a magnetic field is measured and the impressed current density on a conducting plane, the size of the magnetometer pickup coil, and the spatial resolution of the images of the current density. Future capability of varying the above parameters for optimum image resolutions in magnetic inversion technique is principal for future breakthroughs in scientific and medical investigations. More so, with the emerging applications of magnetic inversion technique in virtually every sphere of human endeavours, ranging from, human brain and heart diagnostics, semiconductor physics and nanotechnology, airplane and nuclear plant testing, oil and natural minerals prospecting, and unraveling buried ordnances, among others, advances in imaging techniques will translate to a better-life for humanity.

Corresponding Author: Akala A.O., Email: aandrewakal@unilag.edu.ng, Tel: +2348055419769

Journal of the Nigerian Association of Mathematical Physics Volume 63, (Jan. – March, 2022 Issue), 195 –200

2.0 Formulation of the Problem

Figure 1 shows the formulation of the problem

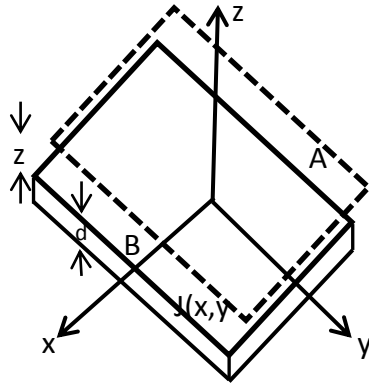


Figure 1: Schematic diagram of the point of observation of current density $\mathbf{J}(\mathbf{r})$ spatially distributed within a thin sheet, B of thickness d in the x - y plane. Magnetic field, $\mathbf{B}(\mathbf{r})$ is measured by a magnetometer over an x - y plane at a height z_0 above the plane of observation A .

The current density is assumed to be quasistatic; hence, its divergence vanishes.

$$\nabla \cdot \mathbf{J} = 0 \tag{1}$$

In electrodynamics, current density and magnetic field are related by the Biot-Savart law, eq. (2);

$$\mathbf{B}(\mathbf{r}) = \frac{\mu_0}{4\pi} \int \frac{\mathbf{J}(\mathbf{r}') \times (\mathbf{r} - \mathbf{r}')}{|\mathbf{r} - \mathbf{r}'|^3} d^3\mathbf{r}' \tag{2}$$

where μ_0 is the permeability of free space, $4\pi \times 10^{-7}$ T.m/A.

Since the axis of observation is z direction, the current density can be represented in two dimensions as $\mathbf{J}(x,y)$. According to Yuan [15], the z component of the magnetic field can be expressed as;

$$B_z(x, y, z) = \frac{\mu_0 d}{4\pi} \int_{-\infty}^{+\infty} \int_{-\infty}^{+\infty} \frac{J_x(x', y')y - J_y(x', y')x}{[(x-x')^2 + (y-y')^2 + (z-z')^2]^{3/2}} dx' dy' \tag{3}$$

Convolution theorem for current density in two dimensions with Green's function in (x, y) and (x', y') domains can allow us to express eqs. (1) and (3) as;

$$k_x j_y(k_x, k_y) + k_y j_x(k_x, k_y) = 0 \tag{4}$$

$$b_z(k_x, k_y, z) = -\left(\frac{\mu_0 d}{2}\right) e^{-z\sqrt{k_x^2 + k_y^2}} \cdot \frac{k_y j_x(k_x, k_y) - k_x j_y(k_x, k_y)}{\sqrt{k_x^2 + k_y^2}} \tag{5}$$

where k_x and k_y are components of wave vector and j_x, j_y , and b_z are the Fourier transform of J_x, J_y , and B_z .

3.0 Numerical and Simulation Scheme

The dimension of the current sheet in Figure 1 is assumed to be $L \times L$ ($16 \mu\text{m} \times 16 \mu\text{m}$). The current sheet was partitioned into N (128) equal squares in both x and y directions, such that we have 128×128 elemental squares in total. For simplicity, N is chosen to be an even number. The area of each elemental square in real space can be written as; $\Delta x \times \Delta y$, such that; $\Delta x = \Delta y = 16/N$. In k -space, the dimension can be written as; $\Delta k_x = \Delta k_y = 2\pi/(N\Delta x)$. Following the method proposed by Roth et al. [11], and modified by Yuan [15], the one dimensional discrete form of the Fast Fourier Transformation (FFT) and inverse FFT (iFFT) are given by:

$$b_z(k_m) = FFT[B_z(x)] = \sum_{n=1}^N B_z(x_n) e^{\frac{2\pi i}{N}(n-1)(m-1)} \tag{6}$$

$$B_z(x_n) = iFFT[b_z(k)] = \frac{1}{N} \sum_{m=1}^N b_z(k_m) e^{-\frac{2\pi i}{N}(n-1)(m-1)} \tag{7}$$

Defining,

$$x_n = (n - 1 - N/2) \cdot \Delta x \tag{8}$$

$$k_m = (m - 1 - N/2) \cdot \Delta k. \tag{9}$$

Summation sign can be used as an approximation of the integral of a Fourier transform;

$$b_z(k_m) = \int B_z(x) e^{ikx} dx = \sum_{n=1}^N B_z(x_n) e^{ik_m \cdot x_n} \cdot \Delta x \tag{10}$$

Substituting eqs. (8) and (9) into eq. (10), we have;

$$b_z(k_m) = L e^{-(m'-1)\pi i} \frac{1}{N} \sum_{n=1}^N B_z(x_n) e^{\frac{2\pi i}{N}(m'-1)(n-1)} = L e^{-(m'-1)\pi i} \cdot iFFT(B_z) \tag{11}$$

where $m' = m - N/2$. Following similar procedure,

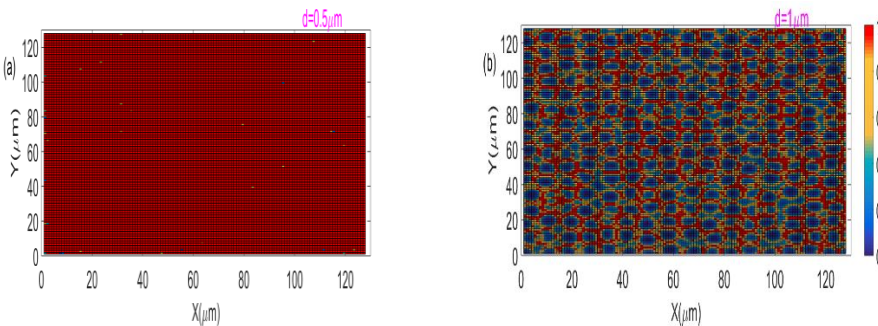
$$J(x_n) = \int j(k) e^{-ikx} dk = \sum_{m=1}^N j_z(k_m) e^{-ik_m \cdot x_n} \cdot \Delta k = \frac{1}{L} e^{(n-1)\pi i} \cdot FFT(j) \tag{12}$$

Eqs. (11) and (12) and their corresponding counterparts in y-direction are then resolved numerically to determine the two-dimensional current density from the associated magnetic field by using MATLAB programming. $J_x(x,y)$ and $J_y(x,y)$ are resolved to reconstruct the current density image $J(x,y)$.

4.0 Results and Discussion

Figure 2 shows the original current density distributions on a square current sheet of area $16 \mu\text{m} \times 16 \mu\text{m}$, at varying thickness; $d = 0.5, 1.0, 1.5, 2.0, 2.5,$ and $3.0 \mu\text{m}$. In Figure 2a, the current sheet density was too low $0.5 \mu\text{m}$, hence, there were basically no well-formed current density map. Figure 2b shows significantly enhanced amplitudes of current density, but blurred images. Whereas, in Figure 2(c & d), the amplitudes of current density were reasonably significant, and the images were most distinct, implying the best resolution of the images among all the panels of Figure 2. On the other hand, Figure (e & f), shows low amplitudes of current density, but sharp images. From Figure 2, it is clear that the thickness of a conducting plane is a major factor that determines its current density distribution and image resolution.

Figure 3 shows the mapping of the magnetic field on a conducting plane of area $16 \mu\text{m} \times 16 \mu\text{m}$, with the magnetic source at varying distances z_0 from conducting plane; $z_0 = 100 \text{ nm}, 100 \mu\text{m}, 100 \text{ mm}$. The results shows good resolution at micrometer and nanometer scales, while the images were blurred for the magnetic field at millimeter scale. Figure 4 is the current identity images reconstructed from the influence of magnetic fields located at varying distances z_0 from conducting plane; $z_0 = 100 \text{ nm}, 100 \mu\text{m}, 100 \text{ mm}$. It was observed, that the spatial resolutions of the reconstructed current density images were high, while the 100 mm magnetic source distance z_0 from conducting plane yielded blurred images, and these images got blurrier and blurrier for $z_0 > 100 \text{ mm}$. Clearer images from any imaging technique imply reliable scientific interpretations of investigations and diagnoses, invariably proffering solutions to human problems [16, 17].



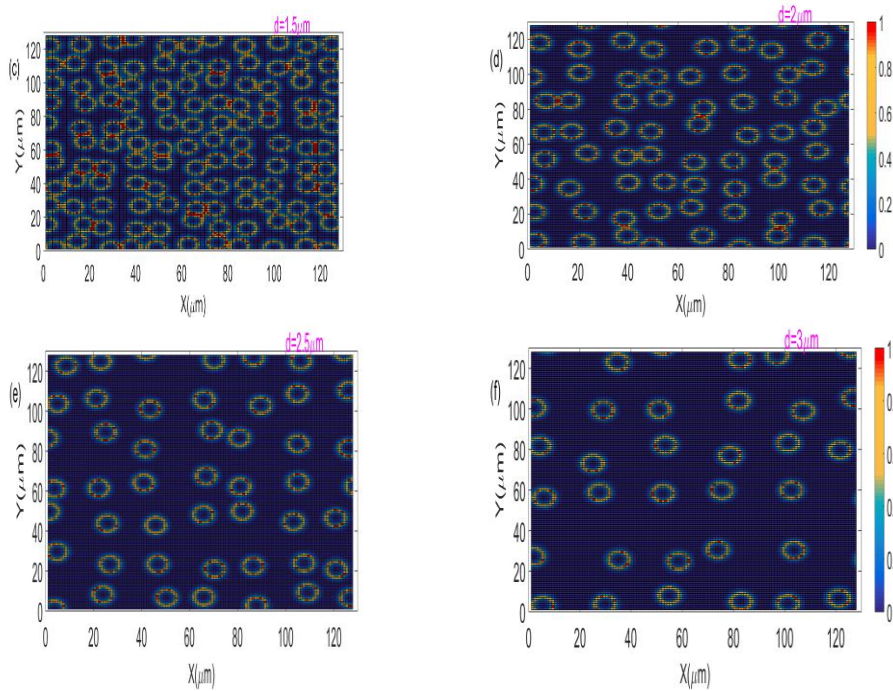


Figure 2: Original current density distributions on a square current sheet of area $16 \mu\text{m} \times 16 \mu\text{m}$, at varying thickness; $d = 0.5, 1.0, 1.5, 2.0, 2.5,$ and $3.0 \mu\text{m}$.

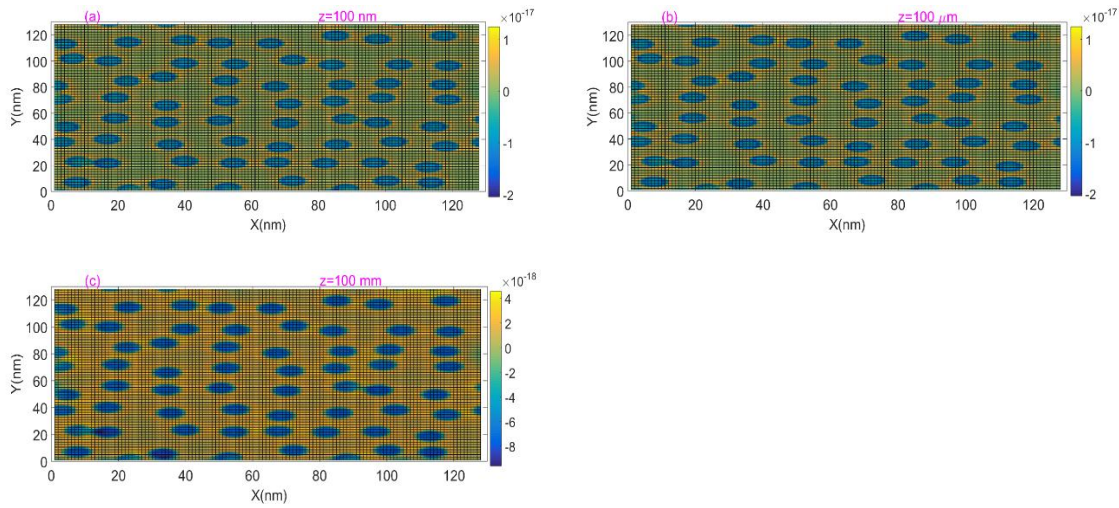
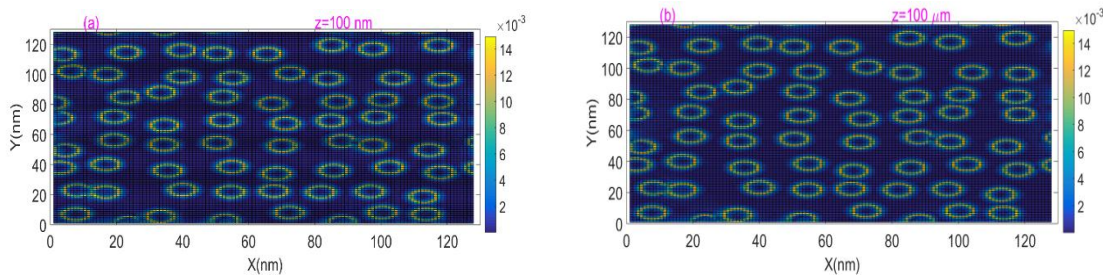


Figure 3 shows the mapping of the magnetic field on a conducting plane of area $16 \mu\text{m} \times 16 \mu\text{m}$, with the magnetic source at varying distances z_0 from conducting plane; $z_0 = 100 \text{ nm}, 100 \mu\text{m}, 100 \text{ mm}$.



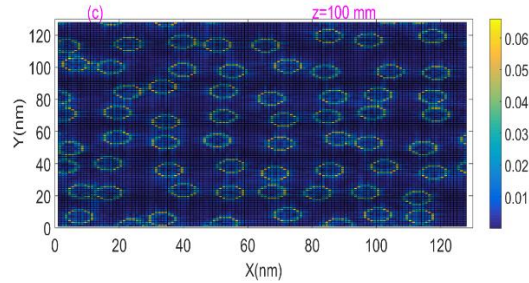


Figure 4: Spatial resolutions of reconstructed current density images from magnetic fields located at varying distances z_0 from conducting plane; $z_0 = 100 \text{ nm}, 100 \mu\text{m}, 100 \text{ mm}$.

5.0 Conclusion

This study solved the magnetic inverse problem via Fourier transforms, and reconstructed a two-dimensional current mapping. The thickness of a conducting sheet determines spatial current density distributions and image resolutions. The spatial resolutions of the reconstructed current density images were higher at nanometer and micrometer scale magnetic source distance to the conducting sheet, and blurred at a millimeter scale distance. Future capabilities that could easily vary the dimensions of a conducting sheet and the distance of the magnetic source plane to the conducting sheet are essential for optimum two dimensional current density image resolutions. This finding is expected to provide support for the improvement of the applications of imaging techniques in scientific investigations and medical diagnoses.

References

- [1] Gans, R. R., R. M. Rose (1993), Crack detection in conducting materials using SQUID magnetometry, *Journal of Nondestructive Evaluation*, 12, 199–207, <https://doi.org/10.1007/BF00568105>
- [2] Baudenbacher, F., N. T. Peters, P. Baudenbacher, J. P. Wikswo (2002), High resolution imaging of biomagnetic fields generated by action currents in cardiac tissue using a LTS-SQUID microscope, *Physica C*, 368, 24–31
- [3] Xing, W., B. Heinrich, H. Zhou, A.A. Fife, A. R. Cragg (1994), Magnetic flux mapping, magnetization, and current distributions of YBa₂Cu₃O₇ thin films by scanning Hall probe measurements *Journal of Applied Physics*, 76, 4244–4255, DOI:10.1063/1.357308.
- [4] Johansen, T. H., M. Baziljevich, H. Bratsberg, Y. Galperin, P. E. Lindelof, Y. Shen, and P. Vase (1996), Direct observation of the current distribution in thin superconducting strips using magneto-optic imaging, *Phys. Rev. B*, 54, 16264–16269
- [5] Schrag, B. D. and G. Xiao (2003), Submicron electrical current density imaging of embedded microstructures, *Applied Physics Letters*, 82(19), 3272–, doi.org/10.1063/1.1570499
- [6] Holzer, J. R., L. E. Fong, V. Y. Sidorov, J. P. Wikswo Jr., and F. Baudenbacher (2004), High Resolution Magnetic Images of Planar Wave Fronts Reveal Bidomain Properties of Cardiac Tissue, *Biophysical Journal*, 87, 4326–4332
- [7] Wang, Z., I. Gutiérrez-Lezama, N. Ubrig, M. Kroner, M. Gibertini, T. Taniguchi, K. Watanabe, A. Imamoğlu, E. Giannini, A. F. Morpurgo (2018), Very large tunneling magnetoresistance in layered magnetic semiconductor CrI₃. *Nature Communication*, 9, 2516, <https://doi.org/10.1038/s41467-018-04953-8>
- [8] Song T., X. Cai, M. W. Tu, X. Zhang, B. Huang, N. P. Wilson, K. L. Seyler, L. Zhu, T. Taniguchi, K. Watanabe, M. A. McGuire, D. H. Cobden, D. Xiao, W. Yao, X. Xu (2018), Giant tunneling magnetoresistance in spin-filter van der Waals heterostructures, *Science*, 15; 360(6394):1214-1218, doi: 10.1126/science.aar4851
- [9] Steinert, S., F. Dolde, P. Neumann, A. Aird, B. Naydenov, G. Balasubramanian, F. Jelezko, and J. Wrachtrup (2010), High sensitivity magnetic imaging using an array of spins in diamond, *Review of Scientific Instruments* 81, 043705, <https://doi.org/10.1063/1.3385689>
- [10] Shibata, Y.; S. Nomura, H. Kashiwaya, S. Kashiwaya, R. Ishiguro, H. Takayanagi (2015), Imaging of current density distributions with a Nb weak-link scanning nano-SQUID microscope. *Scientific Report*, 5, 15097; doi: 10.1038/srep15097.
- [11] Roth, B. J., N. G. Sepulveda, and J. P. Wikswo Jr. (1989), Using a magnetometer to image a two dimensional current distribution, *Journal of Applied Physics*, 65, 361-372, doi: 10.1063/1.342549

- [12] Jiang S., J. Shan, K. F. Mak (2018), Electric-field switching of two-dimensional van der Waals magnets. *Nature Materials*, 17(5):406-410, doi: 10.1038/s41563-018-0040-6
- [13] Klein D. R., D. MacNeill, J. L. Lado, D. Soriano, E. Navarro-Moratalla, K. Watanabe, T. Taniguchi, S. Manni, P. Canfield, J. Fernández-Rossier, P. Jarillo-Herrero (2018), Probing magnetism in 2D van der Waals crystalline insulators via electron tunneling, *Science*, 15;360(6394):1218-1222, doi: 10.1126/science.aar3617.
- [14] Thiel, L., Z. Wang, M. A. Tschudin, D. Rohner, I. Gutiérrez-Lezama, N. Ubrig, M. Gibertini, E. Giannini, A. F. Morpurgo, P. Maletinsky (2019), Probing magnetism in 2D materials at the nanoscale with single-spin microscopy, *Science*, 364 (6444), 973-976, DOI: 10.1126/science.aav6926
- [15] Yuan, Z. (2009), *Quantum Transport in Spatially Modulated Two-dimensional Electron and Hole Systems*, Ph.D. Thesis, Rice University, Huston, Texas, USA.
- [16] Pesikan, P., M. L. G. Joy, G. C. Scott, and R. M. Henkelman (1990), Two-Dimensional Current Density Imaging, *IEEE Transactions on Instrumentation and Measurement*, 39(6), 1048–1053
- [17] Chang, K, A. Eichler, J. Rhensius, L. Lorenzelli, and C. L. Degen (2017), Nanoscale Imaging of Current Density with a Single-Spin Magnetometer, *Nano Letters*, DOI: 10.1021/acs.nanolett.6b05304